Collisional shock waves induced by laser radiation pressure

Zohar Henis[1], Shalom Eliezer[1,2] and Erez Raicher[3]

[1]Physics Division, Soreq Nuclear Research Center, Yavne, Israel; [2]Institute of Nuclear Fusion Guillermo Velarde, Polytechnic University of Madrid, Madrid, Spain and [3]Max-Planck-Institut fur Kernphysik, Saupfercheckweg 1, 69117 Heidelberg, Germany

Abstract

The formation of a collisional shock wave by the light pressure of a short-laser pulse at intensities in the range of 10^{18}–10^{23} W/cm^2 is considered. In this regime the thermodynamic parameters of the equilibrium states, before and after the shock transition, are related to the relativistic Rankine–Hugoniot equations. The electron and ion temperatures associated with these shock waves are calculated. It is shown that if the time scale of energy dissipation is shorter than the laser pulse duration a collisional shock is formed. The electrons and the ions in the shock-heated layer may have equal or different temperatures, depending on the laser pulse duration, the material density and the laser intensity. This shock wave may serve as a heating mechanism in a fast ignition scheme.

Introduction

Upon interaction of lasers with intensity $I_L > 10^{18}$ W/cm^2 and pulse duration $\tau_L < 20$ ps with solid targets the laser radiation pressure may lead to the generation of relativistic shock waves, i.e., the thermodynamic parameters of the equilibrium states are related to the relativistic Rankine–Hugoniot equations. These shock waves may be driven by different mechanisms. One of the models describing these shocks is the laser-piston model. For laser intensities $I_L > 10^{18}$ W/cm^2 the laser ponderomotive force pushes electrons ahead, so that the charge separation field forms a double layer. This double layer structure, called a laser piston, drives a shock compression wave moving in the unperturbed over-dense plasma. The double layer (DL) separates the propagation path of the laser pulse from the shocked plasma. The structure of the piston and the relation between its velocity and the laser intensity were described analytically and as well obtained in particle in cell simulations (Esirkepov *et al.*, 2004; Naumova *et al.*, 2009; Schlegel *et al.*, 2009; Eliezer *et al.*, 2014, 2016; Schmidt and Boine-Frankenheim, 2016). The laser piston as a mechanism of particle acceleration to relativistic velocities was described in papers by Robinson *et al.*, 2009 and Macchi, 2013 and references therein. Two-fluid simulations of laser plasma interaction where the nonlinear ponderomotive force was predominant and was predicted by ultrahigh acceleration of plasma blocks (Hora, 2012).

Shock waves may be divided in two types, depending on the dissipation of kinetic energy at the shock front. In collisional shocks the kinetic energy dissipation is provided by Coulomb binary collisions and as a result the shock front is a few mean free path thick. In collisionless shock waves instabilities due to collective behavior of the plasma or reflection of ions from the shock front provide energy dissipation at the front, and the shock front can be several orders of magnitude smaller than the mean free path for binary collisions. In a high-intensity laser plasma interaction ions are usually heated indirectly by the electrons, ions gain thermal energy through electron ion-thermal equilibration or electron-ion instabilities. For short-pulse laser-induced shock waves an interesting question is whether electrons and ions establish their own post-shock temperature. Bulk heating due to laser piston-induced shock waves is considered here. Hot layer formation by sub-picosecond laser irradiation at intensities higher than 10^{19} W/cm^2 has been reported (Theobald *et al.*, 2006) and described by a model including refluxing and confinement of supra-thermal in target volume. Shock heating of a thin layer at near solid density to 5 keV by $5 \cdot 10^{20}$ W/cm^2 laser radiation pressure driven shock was measured by Akli *et al.*, 2008.

In a recent paper (Eliezer *et al.*, 2017) we considered the shock wave induced by the laser piston propagating into aluminum at normal density, in particular the heating of the material produced during the shock compression, based on energy dissipation by binary collisions. It was shown that the shocked plasma might have different electron and ion temperatures, depending on the laser intensity and duration. In that paper (Eliezer *et al.*, 2017) it was assumed that energy was dissipated at a constant rate. The novel aspects of this paper are based on a new energy dissipation rate where the energy deposition rate is temperature dependent. Furthermore, we extend the model to additional materials and analyze the conditions that allow the formation of a collisional shock wave.

Section "Laser piston-induced relativistic shock wave" presents the relativistic Rankine–Hugoniot equations describing the shock wave in the material and the dependence of the shock parameters on the laser intensity. Section "Thermalization in laser-induced shock waves" proposes a model of the plasma heating produced during the laser piston-induced shock wave. Section "Numerical results" presents the numerical results for deuterium, carbon and aluminum targets and Section "Summary" concludes the paper.

Laser piston-induced relativistic shock wave

The shock wave induced by the laser piston is described by the relativistic Rankine–Hugoniot equations, relating the shock pressure P, energy density e, mass density ρ, particle (piston) velocity u_p and shock velocity u_s. The quantities with subscript zero are the corresponding material parameters before the shock arrival:

$$\frac{u_p}{c} = \sqrt{\frac{(P - P_0)(e - e_0)}{(e_0 + P)(e + P_0)}} \tag{1a}$$

$$\frac{u_s}{c} = \sqrt{\frac{(P - P_0)(e + P_0)}{(e - e_0)(e_0 + P)}} \tag{1b}$$

$$\frac{(e + P)^2}{\rho^2} - \frac{(e_0 + P_0)^2}{\rho_0^2} = (P - P_0)\left[\frac{(e_0 + P_0)}{\rho_0^2} + \frac{(e + P)}{\rho^2}\right] \tag{1c}$$

where c is the speed of light. The velocities u_p and u_s are given in the laboratory frame of reference.

The relativistic shock wave of Eq. (1) yields the following non-relativistic well known Hugoniot equations, when the velocities v satisfy $v/c \ll 1$, and $e = \rho c^2 + \rho E$, where P and ρE are much smaller than ρc^2:

$$u_p = \left(\frac{1}{\rho_0} - \frac{1}{\rho}\right)^{1/2}(P - P_0)^{1/2} \tag{2a}$$

$$u_s = \frac{1}{\rho_0}\left(\frac{1}{\rho_0} - \frac{1}{\rho}\right)^{-1/2}(P - P_0)^{1/2} \tag{2b}$$

$$E - E_0 = \frac{1}{2}\left(\frac{1}{\rho_0} - \frac{1}{\rho}\right)(P + P_0) \tag{2c}$$

We assume an ideal equation of state (EOS)

$$e\left[\frac{\text{erg}}{\text{cm}^3}\right] = \rho c^2 + \frac{P}{\Gamma - 1} \tag{3}$$

$\Gamma = (c_p/c_v)$ is the specific heat ratio related to the number of degrees of freedom per particle f by $\Gamma = 1 + (2/f)$. We assume $\Gamma = (5/3)$, $f = 3$. In the non-relativistic limit the above EOS is

$$E\left[\frac{\text{erg}}{\text{g}}\right] = \frac{P}{\rho(\Gamma - 1)}.$$

The laser piston velocity u_p, or $\beta_p = (u_p/c)$, as a function of the laser intensity I_L can be obtained by solving the relativistic Rankine–Hugoniot equation (1) together with the piston model equation:

$$P = \frac{2I_L}{c}\frac{1 - \beta_p}{1 + \beta_p} \tag{4}$$

where P is the radiation pressure equal to the shock pressure. The relativistic Rankine–Hugoniot equations are solved below for dimensionless variables: compression $\kappa = (\rho/\rho_0)$, dimensionless pressure $\Pi = (P/\rho_0 c^2)$ and dimensionless laser intensity $\Pi_L = (I_L/\rho_0 c^3)$ (Eliezer *et al.*, 2014).

Substituting the ideal EOS [Eq. (3)] with the Rankine–Hugoniot equation (1), we obtain the relativistic Hugoniot equation for dimensionless variables:

$$\Pi^2 + B\Pi + C = 0 \tag{5}$$

$$\Pi = \frac{-B + \sqrt{B^2 - 4C}}{2} \tag{6}$$

$$B = \frac{(\Gamma - 1)^2}{\Gamma}(\kappa_0\kappa - \kappa^2) + \Pi_0(\Gamma - 1)(1 - \kappa^2) \tag{7}$$

$$C = \frac{(\Gamma - 1)^2}{\Gamma}(\kappa - \kappa_0\kappa^2)\Pi_0 - \kappa^2\Pi_0^2 \tag{8}$$

In Eqs. (7, 8) $\kappa_0 = (\Gamma + 1/\Gamma - 1)$ is the non-relativistic asymptotic compression in the limit of infinite shock pressure and $\Pi_0 = (P_0/\rho_0 c^2)$. The solution of the Hugoniot equations for dimensionless variables is material and initial density independent.

We consider here the dimensionless pressure regime:

$$10^{-6} \leq \Pi \leq 10^{-2} \tag{9}$$

This regime corresponds to piston velocities in the range of 0.001–$0.1c$. The compression as a function of the dimensionless pressure, obtained from solving Eqs. (1, 3) is shown in Figure 1a and a zoom displaying the range considered here is shown in Figure 1b. The non-relativistic shock wave regime corresponds to compressions less than four, followed by an intermediate regime where the compression increases very slowly, while the pressure increases by about 10 orders of magnitude and a relativistic regime where there is no upper limit to the compression, unlike for the non-relativistic Hugoniot Eq. (2). The laser intensities generating the pressures considered here are from several times 10^{17} W/cm^2 to 10^{22} W/cm^2, depending on the material initial density. Figure 2 shows the piston/particle and the shock velocity as a function of laser intensity, obtained from the solution of the relativistic Hugoniot equation (1) coupled to the laser piston relation (4), for material initial density $\rho_0 = 1$ g/cm^3. Increasing the initial density shifts the laser intensities linearly to higher values for the same piston velocity.
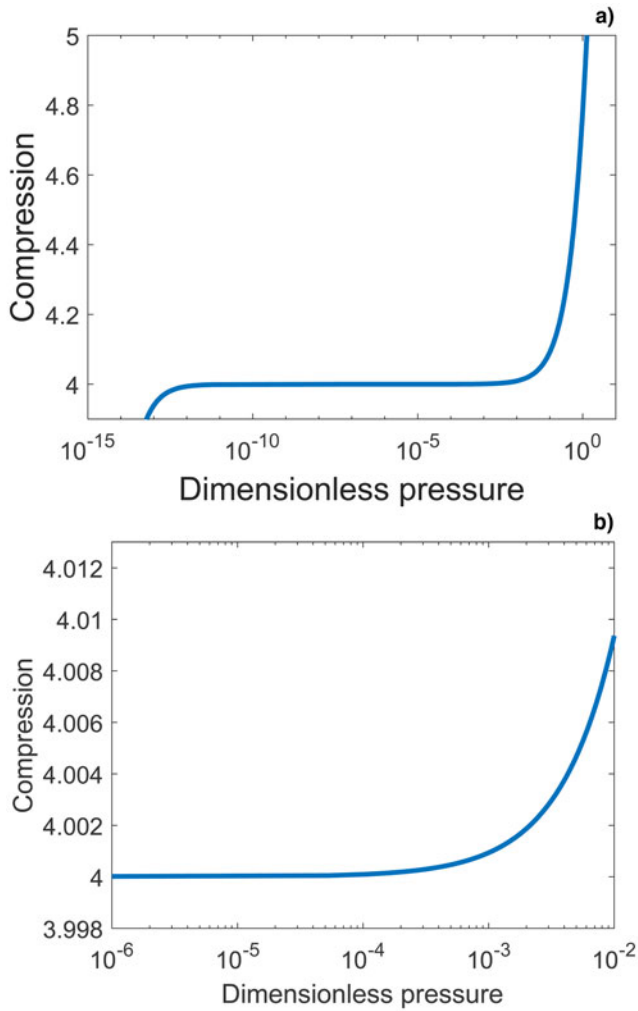
Fig. 1. (a) The compression $\kappa = (\rho/\rho_0)$ as a function of the normalized, dimensionless pressure, $\Pi = (P/\rho_0 c^2)$., for $\Gamma = (5/3)$. (b) Zoom of (a), displaying the compression as a function of the normalized pressure in the pressure regime considered here.

Thermalization in laser-induced shock waves

Due to the shock wave formation in the material, the ions and the electrons behind the shock front are moving with the piston velocity u_p. For non-relativistic, and/or nanosecond or longer time duration shock waves the piston work is divided equally to kinetic energy $\int (\rho u_p^2/2)dV$ and an increase in internal/thermal energy $\int \frac{3}{2} k_B(n_e T_e + n_i T_i)dV$ (Zeldovich and Raizer 1966). For relativistic and semi-relativistic regimes or shorter laser pulse duration the shocked plasma may have in general different ion and electron shock temperatures, T_i and T_e (Eliezer et al., 2015). Moreover, for extremely short-laser pulse duration and high-laser intensity, the ions might not have enough time to achieve thermalization among themselves during the shock duration. The electrons reach thermalization at time shorter than the time scales considered here. Therefore, the laser piston work may be partitioned differently between kinetic and internal energy. In this paper we address this issue, estimating the time of temperature equilibration among the ions and the time of temperature equilibration between the electrons and the ions. It is shown that for given laser intensity there is a threshold pulse duration for the formation of a shock wave. In addition, dependent on the laser
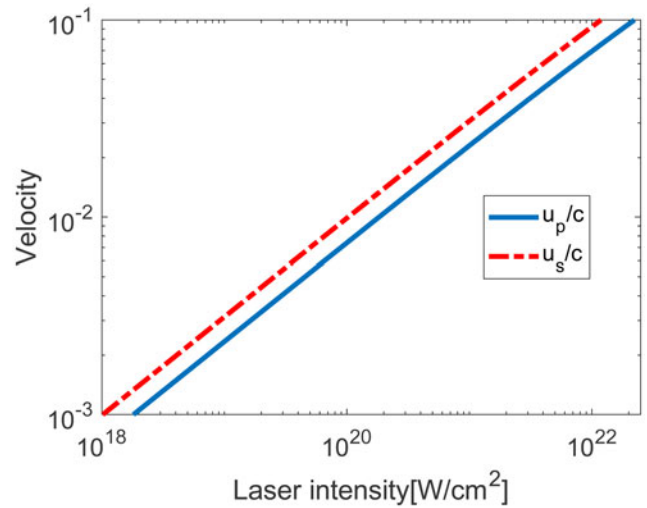
Fig. 2. The particle and shock velocities in units of the velocity of light given by the laser piston model as a function of the laser intensity for initial density $\rho_0 = 1$ g/cm^3, for $\Gamma = (5/3)$.

intensity, the electron and ion temperatures at the end of the pulse duration may be different.

The time-dependent equations for the electron and ion temperatures T_e and T_i are obtained from the energy conservation of the electrons and the ions:

$$\frac{d}{dt}\left(\frac{3}{2}n_e k_B T_e\right) = W_{ie} - W_B + W_d^e \cdot \nu_\varepsilon^{e/e} + W_d^i \cdot \nu_\varepsilon^{i/e} \quad (10)$$

$$\frac{d}{dt}\left(\frac{3}{2}n_i k_B T_i\right) = -W_{ie} + W_d^e \cdot \nu_\varepsilon^{e/i} + W_d^i \cdot \nu_\varepsilon^{i/i} \quad (11)$$

The electron and ion densities are n_e and n_i, and k_B is the Boltzmann constant. W_{ie} (erg/cm^3 s) is the rate of the electron–ion exchange energy density and W_B (erg/cm^3 s) is the appropriate bremsstrahlung losses of the electron energy density. The energy deposition into the ions W_d^i(erg/cm^3) and the electrons W_d^e(erg/cm^3) is obtained from the piston work. It is important to point out that the upper limit of $W_d^i + W_d^e$ equals 50% of the piston energy density. $\nu_\epsilon^{\alpha/\beta}$ is the rate of energy loss of test particles α in a background of field particles β. α, β = e, i. These rates are density, temperature, and velocity dependent.

The bremsstrahlung power loss term is:

$$W_B\left[\frac{erg}{cm^3 s}\right] = 1.25 10^{-25} n_e n_i Z_{av}^2 T_e^{0.5}\left(1 + \frac{2T_e}{0.511 \cdot 10^6}\right) \quad (12)$$

Here the electron temperature is in eV units and Z_{av} is the average ionization in the material.

The temperature equilibration term between the electrons and the ions is:

$$W_{ie}\left[\frac{erg}{cm^3 s}\right] = \frac{3}{2}n_e k_B \frac{(T_i - T_e)}{\tau_{eq}} \quad (13)$$

The electron ion thermal equilibration time τ_{eq} is given by:

$$\tau_{eq} = \frac{3m_e m_i}{8(2\pi)^{1/2}} \frac{1}{n_i Z_{av}^2} \frac{1}{e^4 \ln\Lambda}\left(\frac{k_B T_e}{m_e} + \frac{k_B T_i}{m_i}\right)^{3/2} \quad (14)$$

where m_e and m_i are the electron and ion masses and e is the electron charge.

From the fact that 50% of the piston work can contribute to thermal energy and other losses we obtain

$$W_d \left[\frac{erg}{cm^3}\right] = W_d^i + W_d^e = \frac{Pu_p}{2(u_s - u_p)} = \frac{\rho u_p^2}{2} \quad (15)$$

The last part of Eq. (15) results from the non-relativistic Hugoniot conservation equations.

The deposited energy W_d is calculated after solving the Hugoniot relativistic equations for the pressure and the particle and shock velocities as a function of the laser intensity.

We consider the energy deposition to the electrons and the ions, as test particles and as field particles, separately. The energy deposition is distributed according to the electron and ion masses.

$$W_d^i = \frac{W_d}{(1 + (n_e m_e / n_i m_i))} \quad (16)$$

$$W_d^e = W_d - W_d^i \quad (17)$$

$$W_d \left[\frac{erg}{cm^3}\right] = \frac{\rho u_p^2}{2} - \int W_B dt \quad (18)$$

Due to the large ion-electron mass ratio $W_d^i \gg W_d^e$.

Assuming that the laser pulse rise time is very small in comparison with the laser pulse duration, at the shock wave front the target particle velocity changes instantaneously from zero to a velocity u_p. This is equivalent to a shock wave rise time much shorter than the laser pulse duration. We consider here collisional shock waves, i.e., we assume that the time equilibrations to reach the temperatures $T_e(t < \tau_L)$ and $T_i(t < \tau_L)$ are obtained by Coulomb binary collisions near the shock wave front. In this model we describe the piston energy deposition of the shocked particles, electrons, and ions into thermal energy using a relaxation rate arising from the interaction of test particles, labeled α, streaming with velocity u_p, through a background of field particles, labeled β with a collision frequency of energy deposition (Huba 2011) given by:

$$\nu_\varepsilon^{\alpha/\beta} = 2\left[\frac{m_\alpha}{m_\beta}\psi(x^{\alpha/\beta}) - \psi'(x^{\alpha/\beta})\right]\nu_0^{\alpha/\beta} \quad (19)$$

Here α and β stand for the electrons or ions, α/β denotes kinetic energy transferred from test α to field β particles, m_α and m_β stands for the electron and ion mass, $\nu_0^{\alpha/\beta}$, the relaxation rate scale and the function ψ are defined by

$$\nu_0^{\alpha/\beta} = 4\pi q_\alpha^2 q_\beta^2 \lambda_{\alpha\beta} n_\beta / m_\alpha^2 v_\alpha^3 \quad (20)$$

$$x^{\alpha/\beta} = \frac{m_\beta v_\alpha^2}{2k_B T_\beta} \quad (21)$$

$$\psi(x) = \frac{2}{\sqrt{\pi}} \int\limits_0^x dt\, t^{1/2} e^{-t} \quad (22)$$

$$\psi'(x) = \frac{d\psi}{dx} \quad (23)$$

T_β denotes the temperature of the field particles, v is the test particle velocity, $v = u_p$, q_α and q_β are the charges (q equals the electron charge e for the electrons and $Z_{av}e$ for the ions), and k_B is the Boltzmann constant. $\lambda_{\alpha\beta} = \ln \Lambda_{\alpha\beta}$ is the Coulomb logarithm. The transfer rate $\nu_\varepsilon^{\alpha/\beta}$ is positive for $\varepsilon > \varepsilon_\alpha^*$, and negative for $\varepsilon < \varepsilon_\alpha^*$, where $\varepsilon = (1/2)m_\alpha v_\alpha^2$ and $x^* = (m_\beta/m_\alpha)(\varepsilon_\alpha^*/T_\beta)$ are the solution of $\psi'(x^\star) = (m_\alpha/m_\beta)\psi(x^\star)$. Eq. (20) indicates that the energy transfer rates increase linearly with the density and the average ionization and decrease with increasing piston velocity.

The timescale for energy dissipation is related to the collision mean free path. For ion–ion collisions the mean free path is (Huba, 2011):

$$l_{ii} = \frac{3\sqrt{6}}{8} \frac{m_i^2 u_p^4}{\pi Z^4 e^4 n_i \ln\Lambda} = \frac{u_p}{\nu_0^{i/i}} \quad (24)$$

The average ionization Z_{av} is obtained from the calculation of population of the ionization stages as a function of time:

$$\frac{dn_z}{dt} = n_e(n_{z-1}S_z - n_z S_{z+1} - n_z R_z + n_{z+1}R_{z+1}) \quad (25)$$

where S_z is the ionization coefficient for creating an ion with charge z, R_z is the recombination coefficient of an ion with of charge z, $n_e = \sum_{z=1}^{Z} z n_z$ is the electron density, and Z is the atomic number.

Analytical expressions for the ionization and recombination rates and values of the ionization potentials of aluminum are given in the Appendix.

The $(Z + 1)$ equations for the ionization states (including the neutral) are solved together with the ion and electron temperatures as a function of time.

The formation of a shock wave requires that the spatial scale of the shocked region is larger than the spatial scale of the shock front width, setting a lower limit on the laser pulse duration τ_L

$$(u_s - u_p) \cdot \tau_L \gg \tau_R u_s \quad (26)$$

where the relaxation time τ_R is

$$\tau_R = \max(\tau_e, \tau_i) \quad (27)$$

$$\tau_e = \frac{1}{\nu_\varepsilon^{e/e} + \nu_\varepsilon^{e/i}} \quad (28)$$

$$\tau_i = \frac{1}{\nu_\varepsilon^{i/e} + \nu_\varepsilon^{i/i}} \quad (29)$$

Equivalent to Eq. (26), the spatial scale of the shocked region must be larger than the ion–ion mean free path:

$$l_{ii} < (u_s - u_p)\tau_L. \quad (30)$$

Therefore, a lower limit on the laser pulse duration is:

$$\frac{\tau_R u_s}{u_s - u_p} < \tau_L \quad (31)$$

Table 1. Particle velocity, compressibility and dimensionless pressure, and laser intensity for laser piston-induced shock waves. The shock velocity is $u_s = 4/3 u_p$ for $\Gamma = 5/3$

u_p	κ	Π	Π_L
$0.001c$	4.0000013	$1.39 \cdot 10^{-6}$	$6.97 \cdot 10^{-7}$
$0.01c$	4.000125	$1.333 \cdot 10^{-4}$	$6.8 \cdot 10^{-5}$
$0.1c$	4.0126	0.0135	0.0082

Table 2. Pressure, laser intensity, ion–ion and ion–electron energy loss rate scales for deuteron at normal liquid density $\rho_0 = 0.16$ g/cm^3

u_p	P (erg/cm^3)	I_L (W/cm^2)	$\nu_0^{i/i}$(s^{-1})	$\nu_0^{i/e}$(s^{-1})
$0.001c$	$2.1 \cdot 10^{14}$	$3.16 \cdot 10^{17}$	$2.1 \cdot 10^{12}$	$2.1 \cdot 10^{12}$
$0.01c$	$1.92 \cdot 10^{16}$	$2.98 \cdot 10^{19}$	$2.1 \cdot 10^{9}$	$2.1 \cdot 10^{9}$
$0.1c$	$1.94 \cdot 10^{18}$	$3.55 \cdot 10^{21}$	$2.1 \cdot 10^{6}$	$2.1 \cdot 10^{6}$

Table 3. Pressure, laser intensity, ion–ion and ion–electron energy loss rate scales for carbon at normal density $\rho_0 = 1$ g/cm^3

u_p	P (erg/cm^3)	I_L (W/cm^2)	$\nu_0^{i/i}$(s^{-1})	$\nu_0^{i/e}$(s^{-1})
$0.001c$	$1.25 \cdot 10^{15}$	$1.89 \cdot 10^{18}$	$7.9 \cdot 10^{13}$	$1.3 \cdot 10^{13}$
$0.01c$	$1.2 \cdot 10^{17}$	$1.\,83 \cdot 10^{20}$	$7.9 \cdot 10^{10}$	$1.3 \cdot 10^{10}$
$0.1c$	$1.21 \cdot 10^{19}$	$2.2 \cdot 10^{22}$	$7.9 \cdot 10^{7}$	$1.3 \cdot 10^{7}$

Table 4. Pressure, laser intensity, ion–ion and ion–electron energy loss rate scales for aluminum at normal density $\rho_0 = 2.7$ g/cm^3

| u_p	P (erg/cm^3)	I_L (W/cm^2)	$\nu_0^{i/i}$(s^{-1})	$\nu_0^{i/e}$(s^{-1})
$0.001c$	$3.38 \cdot 10^{15}$	$5. \cdot 10^{18}$	$4.1 \cdot 10^{14}$	$3.1 \cdot 10^{13}$
$0.01c$	$3.24 \cdot 10^{17}$	$4.95 \cdot 10^{20}$	$4.1 \cdot 10^{11}$	$3.1 \cdot 10^{10}$
$0.1c$	$3.27 \cdot 10^{19}$	$6. \cdot 10^{22}$	$4.1 \cdot 10^{8}$	$3.1 \cdot 10^{7}$

Table 5. Estimated range of the laser pulse duration for the formation of a collisional shock wave

u_p	τ_L – lower limit (s)		
	D	C	Al
$0.001c$	$9.5 \cdot 10^{-13}$	$4.3 \cdot 10^{-14}$	$9. \cdot 10^{-15}$
$0.01c$	$9.5 \cdot 10^{-10}$	$4.3 \cdot 10^{-11}$	$9. \cdot 10^{-12}$
$0.1c$	$9.5 \cdot 10^{-7}$	$4.3 \cdot 10^{-8}$	$9. \cdot 10^{-9}$

Eqs. (10, 11, 24) are numerically integrated up to a time equal to the laser pulse duration.

Numerical results

The following values for the laser piston velocity are considered, $0.001c$, $0.01c$, and $0.1c$. The corresponding shock velocity and compressibility, dimensionless pressure and laser intensity obtained from solving Eqs. 4–8 are given in Table 1.

The laser intensities, pressure and relaxation rate scales $\nu_0^{i/i}$ and $\nu_0^{i/e}$ for deuteron, carbon, and aluminum at normal density are given in Tables 2–4. The relaxation rate scales $\nu_0^{e/e}$ and $\nu_0^{e/i}$ are not shown, as $W_d^i \gg W_d^e$. The relaxation rate scales were calculated assuming that the plasma is fully ionized.

From Eq. (31) and Tables (2–4) it is seen that the formation of a collisional shock wave during the laser pulse duration is not possible for all the materials and the laser piston velocities considered here. From the energy loss rate scales one may approximate the relaxation time τ_R and obtain an estimate for the lower limit for the laser pulse duration. Table 2 shows that the relaxation time for liquid deuterium at piston velocities of $0.01c$ and $0.1c$ is of the order of hundreds of picoseconds and hundreds of nanoseconds, respectively. Therefore, the piston work cannot be transferred into thermal energy of the shocked material on a time scale of few picoseconds. Tables 3 and 4 show that there is no time for piston work deposition in carbon and aluminum at a piston velocity of $0.1c$. In other words, the formation of a collisional shock wave is not possible under the above conditions. A lower limit for the laser pulse duration that may allow the formation of a collisional shock wave, resulting from Eq. (31) and estimated with relaxation time scales, is given in Table 5. This estimate is dependent on the material density and atomic number. The temperature-dependent part of the relaxation rates $\nu_\varepsilon^{i/i}$ and $\nu_\varepsilon^{i/e}$ [Eq. (19)] may shift the value for this lower limit.

The energy loss rates may be increased by the material pre-compression as seen from Eq. (20), and decrease the value of the lower limit for the pulse duration given in Table 5. However, an increase in the initial density will require higher laser intensity.

Solving the electron and the ion temperatures, Eqs. (10, 11) are not dependent on the laser pulse duration. The figures below show the results of the rate equations during a run time of 10 ps.

Figure 3 shows the results of Eqs. (10, 11) for deuterium at liquid normal density at piston velocity $u_p = 0.001c$. The electron and ion temperatures as a function of time are shown in Figure 3a, the energy transfer rates [Eq. (21)] in Figure 3b, and the available energy for deposition $W_d - n_i k_B T_i - n_e k_B T_e$ in Figure 3c. It is seen that the energy deposition ends after about 40 fs, when the ion temperature is 0.48 keV and then the ions and the electrons reach equilibrium at about 0.35 keV after about 10 ps. Therefore, an equilibrium shock wave can be generated. For a piston velocity $u_p = 0.01c$, only 13% of the piston work is deposited during a reference time duration of 10 ps, and the ions do not thermalize. Increasing the density to 10 g/cm^3 enables thermalization of the ions after 3.6 ps to a temperature $T_{imax} = 43.8$ keV, while the electrons are heated to $T_{emax} = 18.4$ keV at this time. Therefore, a non-equilibrium shock wave is generated. Figure 4 shows the electron and ion temperatures and the energy transfer rates for initial density 10 g/cm^3 and $u_p = 0.01c$. After the piston work deposition, thermal energy is transferred from the ions to the electrons at a rate of $1/\tau_{eq}$ [Eq. (14)].

Figure 5 shows the electron and ion temperatures and the energy transfer rates for carbon at initial density $\rho_0 = 1$ g/cm^3 and piston velocity $u_p = 0.01c$. It is seen that a non-equilibrium shock wave is generated. The maximum ion temperature is about 250 keV at 4.6 ps when the piston work deposition ends. From the energy loss rates displayed in Figure 5b, the relaxation time τ_R is 6.7 ps [Eq. (30)].
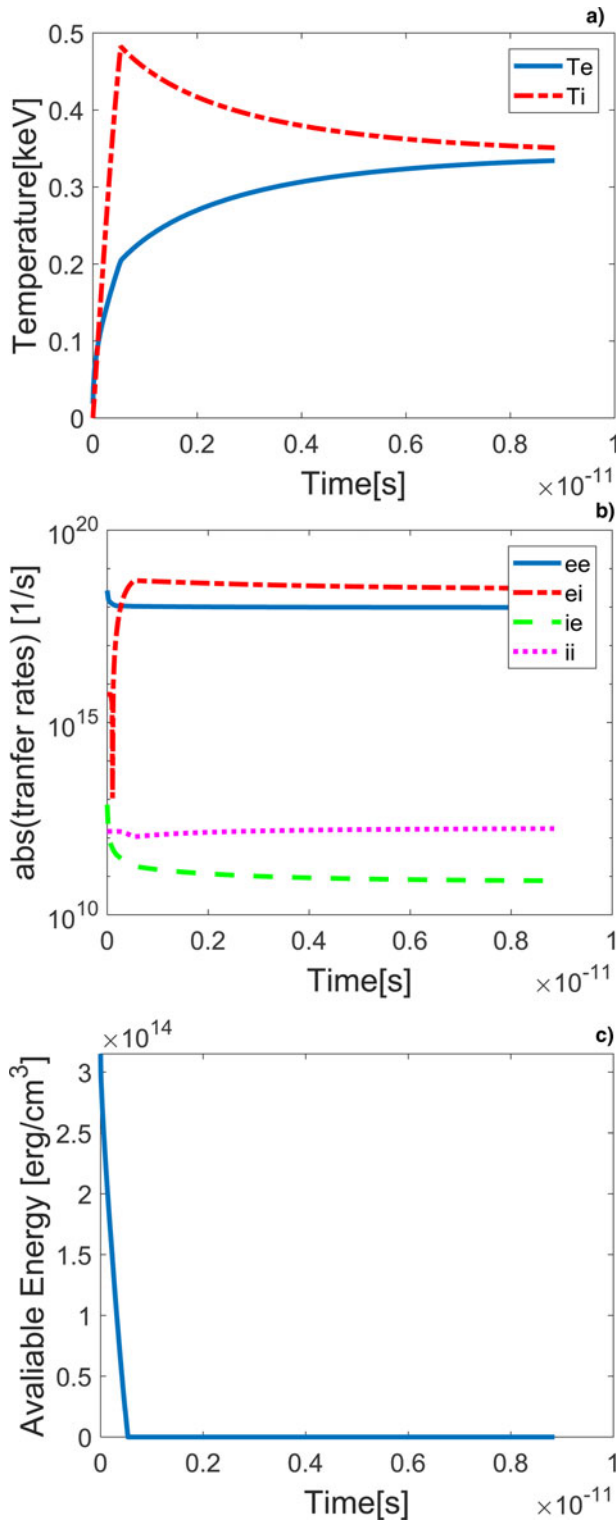
Fig. 3. (a) Numerical results for liquid deuterium, $\rho_0 = 0.16$ g/cm^3, $u_p = 0.001c$. Electron (solid line) and ion (dashed line) temperatures as a function of time. (b) Absolute value of the energy transfer rates $v_\varepsilon^{\alpha/\beta}$, e/e – solid line, e/i – dash-dotted line, i/e – dashed line, and i/i – dotted line. (c) Available piston work in (erg/cm^3) for deposition as a function of time.

Similar calculations for aluminum at normal density show the formation of an equilibrium shock wave at piston velocity $u_p = 0.001c$, i.e. the electrons and the ions reach temperature equilibration during the shock wave, and a non-equilibrium
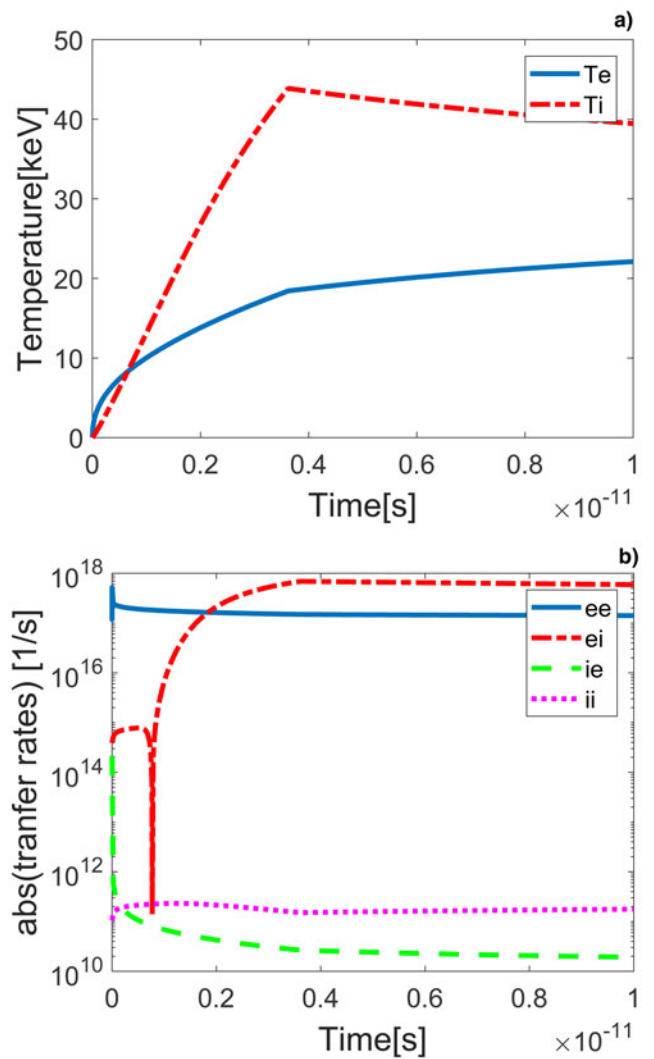
Fig. 4. (a) Numerical results for liquid deuterium, $\rho_0 = 10$ g/cm^3, $u_p = 0.01c$. Electron (solid line) and ion (dashed line) temperatures as a function of time. (b) Absolute value of the energy transfer rates $v_\varepsilon^{\alpha/\beta}$, e/e – solid line, e/i – dash-dotted line, i/e – dashed line, and i/i – dotted line.

shock wave at $u_p = 0.01c$. Figure 6 shows the electron and ion temperatures, energy deposition rates, and piston work deposition as a function of time for normal density and piston velocity $u_p = 0.1c$. In this case there is no time for collisional shock generation on a time scale of about 10 ps.

We note that to obtain a one-dimensional shock wave, the spot size must be larger than l_s the spatial scale of the shocked region:

$$2 \cdot r_L > l_s = (u_s - u_p) \cdot \tau_L \tag{32}$$

From Eq. (32) an estimate for the laser pulse energy is $E_L = \pi r_L^2 \tau_L^3 I_L \geq (\pi/36) u_p^2 \tau_L^3 I_L$.

Summary

The formation of a collisional shock wave by the light pressure of a short-pulse laser at relativistic intensities and the subsequent heating of a solid layer are considered. The heating model is based on the dissipation of kinetic energy by binary Coulomb
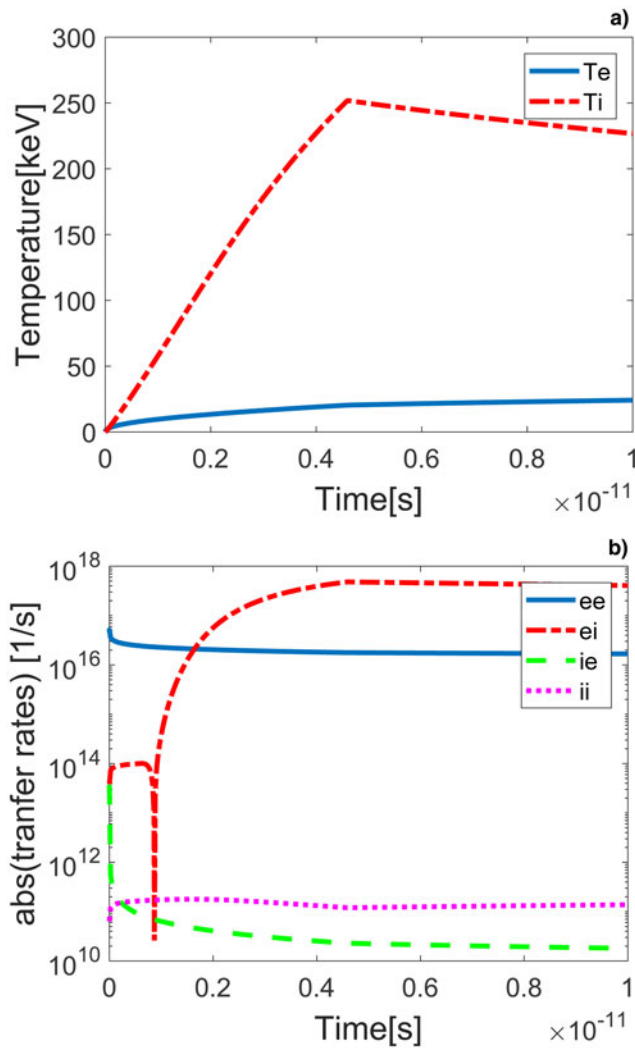
Fig. 5. (a) Numerical results for carbon, $\rho_0 = 1$ g/cm^3, $u_p = 0.01c$. Electron (solid line) and ion (dashed line) temperatures as a function of time. (b) Absolute value of the energy transfer rates $\nu_\varepsilon^{\alpha/\beta}$, e/e – solid line, e/i – dash-dotted line, i/e – dashed line, and i/i – dotted line.

collisions at a temperature-dependent rate. We consider laser intensities in the range of 10^{18} W/cm^2 to 10^{23} W/cm^2 for deuterium, carbon, and aluminum targets. It is obtained that the formation of a collisional shock wave is dependent on the laser intensity and the material density. In the framework of the model presented here three cases were distinguished. If the timescale for energy dissipation is shorter than the laser pulse duration a collisional shock wave can be formed, during which the electrons and the ions either may have different temperatures – nonequilibrium shock wave, or may reach equilibrium at equal temperature. In both equilibrium and non-equilibrium shock waves, at early times the electrons are heated by energy transfer from the ions, and eventually the ion temperature overtakes. A third possibility may occur when the timescale for energy dissipation is longer than laser pulse duration, or the ion–ion collision mean free path l_{ii} is larger than the shock width l_s. In this case a collisional shock wave is not formed. The collisional shock wave described here may serve as a heating mechanism for a fast ignition scheme. In such a scheme deuterium fuel compressed by nanosecond laser pulses to a density by three orders of
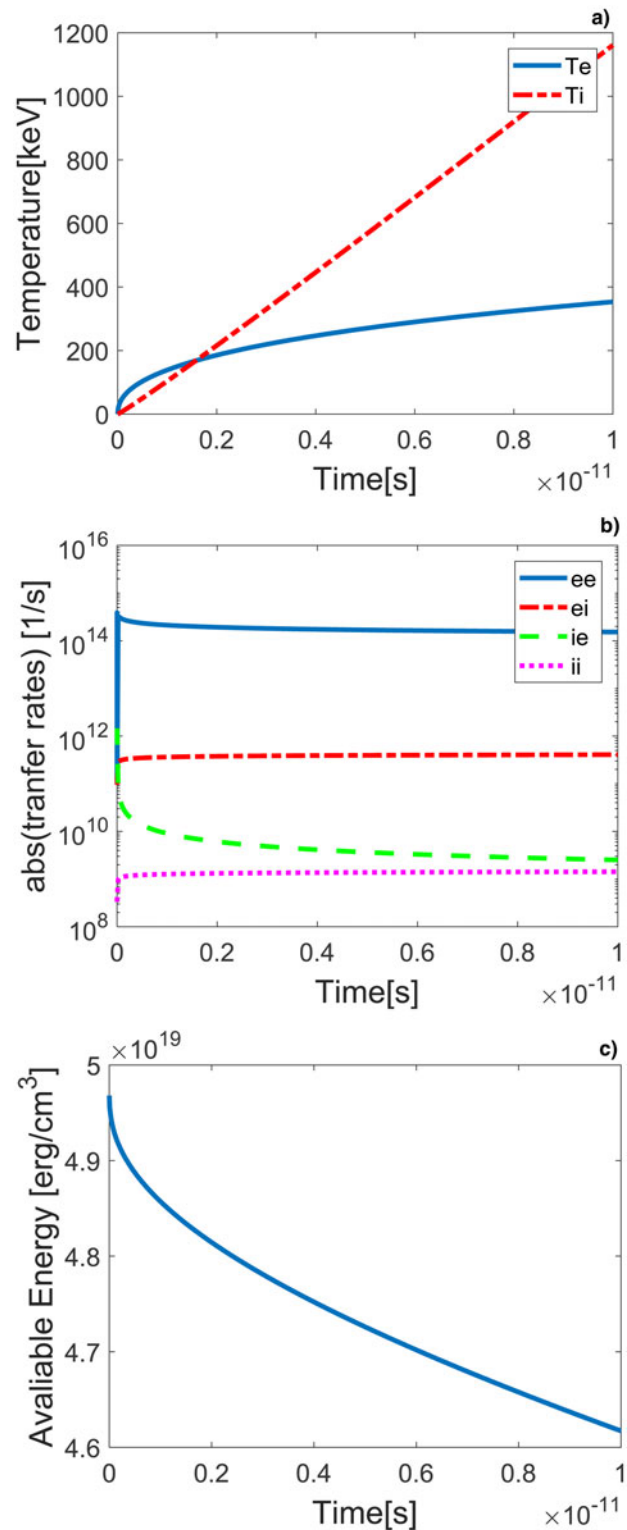
Fig. 6. (a) Numerical results for aluminum, $\rho_0 = 2.7$ g/cm^3, $u_p = 0.1c$. Electron (solid line) and ion (dashed line) temperatures as a function of time. (b) Absolute value of the energy transfer rates $\nu_\varepsilon^{\alpha/\beta}$, e/e – solid line, e/i – dash-dotted line, i/e – dashed line, and i/i –dotted line. (c) Available piston work in erg/cm^3 for deposition as a function of time.

magnitude higher than normal liquid density can be heated by the a shock wave generated by the radiation pressure of 1 ps duration laser at several times its intensity of 10^{23} W/cm^2.

Author ORCIDs. Zohar Henis, https://orcid.org/0000-0001-6813-1400.

References

Akli KU, Hansen SB, Kemp AJ, Freeman RR, Beg FN, Clark DC, Chen SD, Hey D, Hatchett SP, Highbarger K, Giraldez E, Green JS, Gregori G, Lancaster KL, Ma T, MacKinnon AJ, Norrey P, Patel J, Shearer C, Stephens RB, Stoeckl C, Storm M, Theobald W, Van Woerkom LD, Weber R and Key MH (2008) Laser Heating of Solid Matter by Light-Pressure-Driven Shocks at Ultrarelativistic Intensities. *Physical Review Letters* **100**, 165002.

Eidmann K (1994) Radiation transport and atomic physics modeling in high energy density laser produced plasmas. *Laser and Particle Beams* **12**, 223.

Eliezer S, Nissim N, Raicher E and Martinez Val JM (2014) Relativistic shock waves induced by ultra-high laser pressure. *Laser and Particle Beams* **32**, 243–251.

Eliezer S, Henis Z, Nissim N, Pinhasi SV and Martinez Val JM (2015) Introducing a two temperature plasma ignition in inertial confined targets under the effect of relativistic shock waves: the case of DT and pB11. *Laser and Particle Beams* **33**, 577–589.

Eliezer S, Martinez-Val JM, Henis Z, Nissim N, Pinhasi SV, Ravid A, Werdiger M and Raicher E (2016) Physics and applications with laser induced relativistic shock waves. *High Power Laser Science and Engineering* **4**, e25.

Eliezer S, Pinhasi V, Martinez-Val JM, Raicher E and Henis Z (2017) Heating in ultraintense laser-induced shock waves. *Laser and Particle Beams* **35**, 304.

Esirkepov T, Borghesi M, Bulanov SV, Mourou G and Tajima T (2004) Highly efficient relativistic ion generation in the laser piston regime. *Physical Review Letters* **92**, 175003/1–4.

Hora H (2012) Fundamental difference between picosecond and nanosecond laser interaction with plasmas: Ultrahigh plasma block acceleration links with electron collective ion acceleration of ultra-thin foils. *Laser and Particle Beams* **30**, 325.

Huba JD (2011) NRL plasma formulary.

Macchi A (2013) Ion acceleration by super-intense laser plasma interaction. *Reviews of Modern Physics* **85**, 751.

Naumova N, Schlegel T, Tikhonchuk VT, Labaune C, Sokolov IV and Mourou G (2009) Hole boring in a DT Pellet and Fast-Ion Ignition with Ultraintense Laser Pulses. *Physical Review Letters* **102**, 025002.

Robinson APL, Gibbon P, Zepf M, Kar S, Evans RG and Bellei C (2009) Relativistically correct hole-boring and ion acceleration by circularly polarized laser pulses. *Plasma Physics and Controlled Fusion* **51**, 024004.

Schlegel T, Naumova N, Tikhonchuk VT, Labaune C, Sokolov IV and Mourou G (2009) Relativistic laser piston: pondermotive ion acceleration in dense plasmas using ultraintense laser pulses. *Physics of Plasmas* **16**, 083103.

Schmidt P and Boine-Frankenheim O (2016) A gas-dynamical approach to radiation pressure acceleration. *Physics of Plasmas* **23**, 063106.

Theobald W, Akli K, Clarke R, Delettrez JA, Freeman RR, Glenzer S, Green J, Gregori G, Heathcote R, Izumi N, King JA, Koch JA, Kuba J, Lancaster K, MacKinnon AJ, Key M, Mileham C, Myatt J, Neely D, Norreys PA, Park H-S, Pasley J, Patel P, Regan SP, Sawada H, Shepherd R, Snavely R, Stephens RB, Stoeckl C, Storm M, Zhang B and Sangster TC (2006) Hot surface line emission and cold K-inner shell emission from petawatt-laser-irradiated Cu foil targets. *Physics of Plasmas* **13**, 043102.

Zeldovich YB and Raizer YP (1966) *Physics of Shock Waves and High Temperature Hydrodynamic Phenomena*. New York: Academic Press Publications.

Appendix: Ionization and recombination rates and ionization potentials

The following analytical expressions for the ionization and recombination rates were used (Eidmann, 1994):

$$S_z = 2.4 \cdot 10^{-6} \Delta_z \frac{T_e^{1/4}}{I_z^{7/4}} e^{-I_z/T_e} \left[\frac{cm^3}{s} \right] \quad (A1)$$

where $I_z[eV]$ is the ionization potential of an ion with charge z, Δ_z is the number of electrons in the last occupied shell of the ion with charge z.

The recombination rate is generally the contribution of three body and radiative recombination:

$$R_{z+1}^3 = 3.9 \cdot 10^{-28} \frac{\xi_{z+1}}{I_Z^{7/4} T_e^{5/4}} \left[\frac{cm^6}{s} \right] \quad (A2)$$

$$R_{z+1}^r = 1.9 \cdot 10^{-14} \frac{I_z}{T_e^{1/2}} \left[\frac{cm^3}{s} \right] \quad (A3)$$

Here ξ_{z+1} is the number of vacancies in the last shell of ion z. In the above ionization and recombination rates T_e is in eV units.

The $(Z+1)$ equations for the ionization states (including the neutral) are solved together with the ion and electron temperatures as a function of time.

The ionization potential in eV of the aluminum ion stages from the NIST Atomic Spectra database was used in the calculations which are: 5.98, 18.82, 28.44, 119.99, 153.82, 190.49, 241.76, 284.64, 330.21, 398.65, 442, 2085, and 2304.14.